

Evidence for Daily and Weekly Periodic Variability in GPT-4o Performance

Paul Tschisgale^{1,*} and Peter Wulff²

¹Leibniz Institute for Science and Mathematics Education, Kiel, Germany

²Ludwigsburg University of Education, Ludwigsburg, Germany

*Corresponding author.

ABSTRACT

Large language models (LLMs) are increasingly used in research both as tools and as objects of investigation. Much of this work implicitly assumes that LLM performance under fixed conditions (identical model snapshot, hyperparameters, and prompt) is time-invariant. If average output quality changes systematically over time, this assumption is violated, threatening the reliability, validity, and reproducibility of findings. To empirically examine this assumption, we conducted a longitudinal study on the temporal variability of GPT-4o's average performance. Using a fixed model snapshot, fixed hyperparameters, and identical prompting, GPT-4o was queried via the API to solve the same multiple-choice physics task every three hours for approximately three months. Ten independent responses were generated at each time point and their scores were averaged. Spectral (Fourier) analysis of the resulting time series revealed notable periodic variability in average model performance, accounting for approximately 20% of the total variance. In particular, the observed periodic patterns are well explained by the interaction of a daily and a weekly rhythm. These findings indicate that, even under controlled conditions, LLM performance may vary periodically over time, calling into question the assumption of time invariance. Implications for ensuring validity and replicability of research that uses or investigates LLMs are discussed.

Keywords: large language models, GPT-4o, periodic variability, performance evaluation, time-series analysis, Fourier analysis

1 Introduction

1.1 Large Language Model Usage Within Scientific Research

Large language models (LLMs) are a specific model class in the field of generative artificial intelligence (AI), specialized in natural language processing and generation. In the last years, there has been rapid progress in LLM development, accompanied by notable improvements in performance on a broad range of language-related tasks^{1,2}.

Given these substantial advances in LLMs, researchers have shown increasing interest in examining their apparent capabilities across diverse domains, thereby treating *LLMs as objects of research*. In this line of research, LLMs are often evaluated using domain-specific examinations across diverse educational levels^{3,4} or established assessment instruments from educational research^{5,6}, with their performance typically benchmarked against that of human participants. In addition, large-scale benchmark datasets have been developed in multiple domains^{7,8}, one prominent example being Humanity's Last Exam, which comprises expert-level questions spanning a broad range of subjects⁹.

Moreover, researchers have increasingly recognized the potential of *LLMs as research tools* to support a wide range of research-related tasks. In particular, LLMs are increasingly adopted in qualitative research, especially for deductive coding^{10,11}. In such applications, the model's output effectively functions as a coding decision by assigning a given text segment to a category from a predefined coding scheme. Correspondingly, commercial qualitative data analysis software (such as NVivo and MAXQDA¹²) has begun to integrate LLM functionality. Beyond qualitative coding, LLM-based approaches are also being explored for data extraction in systematic literature reviews¹³, reflecting a broader trend toward the integration of AI-based tools to enhance research productivity.

An implicit assumption underlying many studies that investigate LLMs as objects of research or employ them as research tools is that LLM performance is time-invariant under fixed conditions. By time invariance, we mean that an LLM's average performance does not systematically depend on when it is queried. For example, in a study of an LLM's mathematical capabilities, the same set of tasks may be solved multiple times under identical conditions, once in the morning and once in the evening. If performance were to differ systematically between these measurement periods, conclusions drawn from a single time point would be unreliable. Analogously, if an LLM's coding quality in qualitative analyses were systematically higher on certain days (e.g., Wednesdays) than on others (e.g., Mondays), this would directly affect reliability, validity, and reproducibility of the resulting research findings. Consequently, the assumption of time invariance in LLM performance should not be taken

for granted and requires empirical validation.

The present study therefore empirically examines the assumption of time invariance by investigating whether LLM performance under fixed conditions on a well-specified task remains stable over an extended period of time, or whether systematic temporal variation can be detected. By testing this assumption, we assess whether potential performance differences across time are negligible or substantial enough to compromise the validity and reproducibility of LLM-related research findings, including both studies of LLM capabilities and studies that employ LLMs as research tools.

1.2 Variability in Large Language Model-Generated Output

Several factors influence the output of an LLM, including the precise model snapshot (i.e., the exact internal version of the model rather than merely its general family or name), decoding hyperparameters (such as temperature), and the user-provided prompt. Depending on the specific LLM, additional hidden system prompts typically further constrain or guide the generation process, as documented, for example, in the system description of GPT-5¹⁴.

Even when all adjustable conditions are held constant, LLMs typically exhibit variability in their outputs, as response generation relies on autoregressive next-token prediction^{15, 16}. In an autoregressive framework, text is generated token by token by sampling each subsequent token from a probability distribution over the model’s vocabulary, conditioned on the input prompt and all previously generated tokens¹⁷. This sampling procedure is directly influenced by decoding hyperparameters such as temperature. Consequently, outputs may differ across repeated queries despite identical fixed conditions. This stochasticity of LLM-generated output is an intentional design feature, as it allows models to balance output quality and diversity and to avoid degenerate or overly repetitive responses.

In light of these considerations, an LLM can be understood as inducing a probability distribution over the space of all possible generated outputs, conditioned on the specific model snapshot, the user prompt, potential hidden system prompts, and decoding hyperparameters. Each generated output thus constitutes a random draw from this distribution, which explains why individual outputs may differ even when the conditioning context remains unchanged. For example, estimates of an LLM’s mathematical capabilities, operationalized as the proportion of correctly solved tasks, may vary across repeated runs. Similarly, coding decisions in LLM-aided qualitative deductive coding may differ across repeated queries. Such capability estimates or assigned codes typically serve as inputs to subsequent empirical analyses, and their inherent variability introduces uncertainty that must be accounted for. Researchers hence commonly either aggregate LLM outputs across multiple runs (e.g., by averaging task scores) or select the most frequently occurring outputs across runs (e.g., by majority voting in qualitative coding), to improve reliability and also reproducibility.

However, this reasoning rests on the implicit assumption that, under fixed conditions, the probability distribution from which outputs are sampled is stable over time, that is, *time-invariant*. In other words, repeated queries to the LLM under identical conditions are assumed to correspond to repeated draws from the same underlying distribution. Under this assumption, LLM-generated outputs at different points in time can be treated as independent samples from a fixed distribution. The law of large numbers then implies that average performance scores across multiple generations, or empirical frequencies of coding decisions, converge to well-defined expected values as the number of samples increases. From this perspective, it is generally advisable to generate multiple outputs per task and to base empirical conclusions on aggregate statistics rather than on single measurements, since an individual measurement may yield an idiosyncratic performance estimate or coding decision that is not representative of the model’s typical behavior.

We now consider the implications of violating this assumption, for instance due to unobserved changes in system-level components or inference infrastructure.

In a first scenario, multiple LLM outputs are sampled under fixed conditions within a *short time window*, such that the underlying output distribution can reasonably be assumed to remain stable during sampling. In this case, the law of large numbers applies, and aggregating multiple outputs yields a robust estimate of average model performance on a given task. However, if another researcher attempts to reproduce this result at a later point in time—using the same model snapshot, hyperparameters, and prompt, but when the underlying output distribution has changed—the resulting performance estimate may systematically differ, despite no observable changes to the experimental setup. Consequently, the original findings would not be reproducible.

In a second scenario, output sampling spans a *longer time window* over which the LLM’s output distribution changes. Under such conditions, increasing the number of sampled outputs does not necessarily improve reliability. Instead, aggregate statistics may lose their interpretability, as they depend strongly on the temporal location of the sampling. For example, sampling may disproportionately reflect periods of relatively high or low model performance, or may average over distinct performance regimes. In such cases, observed averages may obscure systematic temporal variation and yield misleading estimates of overall model performance.

Taken together, these scenarios illustrate that violations of time invariance can compromise validity and reproducibility of LLM-related research findings, even when experimental conditions appear tightly controlled.

1.3 Related Studies

Prior work examining the temporal behavior of generative AI systems, particularly LLMs, largely falls into one of two categories: (1) studies documenting performance changes across model versions or over long time scales, and (2) studies investigating temporal variability under constant model conditions. The first category establishes a general pattern of evolving capabilities in LLMs, while the second directly relates to the assumption of time invariance that motivates this study.

1.3.1 Temporal Evolution of LLM Capabilities

A large body of research has examined how the performance of LLMs evolves over time as new model versions, updates, or releases become available. Evaluation studies indicate that “most capabilities of ChatGPT improve over time except for some abilities, and there exists a step-wise evolving pattern of ChatGPT”¹⁸, a trend that has also been observed across a broader range of LLMs⁹.

For example, Tu et al.¹⁸ documented stepwise performance gains associated with successive ChatGPT updates, a pattern also reported by Ignjatovic et al.¹⁹. Complementing this perspective, Dai et al.²⁰ developed a dynamic evaluation dataset derived from continuously emerging media content and demonstrated that model performance on newly introduced topics declines as training data become outdated, highlighting the dependence of performance on the temporal scope and the recency of training data.

Comparative analyses of specific model releases further illustrate these dynamics. Chen et al.²¹, for instance, showed that GPT-4’s ability to classify prime versus composite numbers differed substantially between the March and June 2023 versions, with the later version exhibiting reduced accuracy. Such shifts are commonly attributed to changes in training data, optimization objectives, or architectural modifications accompanying new releases.

While these studies demonstrate that model performance can vary substantially across versions, they do not directly address whether the outputs of a fixed model instance remain stable over time when all—or at least most—controllable factors, such as model snapshot, prompting, and decoding parameters, are held constant.

1.3.2 Temporal Variability under Fixed Conditions

Anecdotal evidence from user discussions on online platforms suggests that some users perceive periodic or time-dependent fluctuations in LLM performance²². These observations are often attributed to variations in system load resulting from differing usage intensities and, in some cases, to time zone-dependent usage patterns. Moving beyond such informal reports, recent empirical studies have begun to systematically investigate temporal variability in LLM performance under fixed conditions. For example, Gupta et al.²³ evaluated multiple externally hosted LLMs at three time points spaced one month apart using a set of radiology-related questions and observed measurable changes in model performance over time. Complementary evidence was reported (albeit as a side note) by Tschisgale et al.²⁴, who demonstrated that the score distributions assigned to GPT-4o-generated solutions for selected physics problems differed significantly when outputs were generated six weeks apart.

Taken together, these is some evidence indicating that temporal variability may persist even when model versions, prompts, and hyperparameters are held constant. Such variability—distinct from performance changes across model releases—poses a direct challenge for validity and reproducibility of research that investigates or uses LLMs.

1.4 Potential Mechanism Causing Time Invariance

For LLMs deployed on shared or centrally managed server infrastructure, we speculate that time invariance may arise due to periodic patterns in server load that operate on both daily and weekly time scales. Prior work has shown that real-world usage of large-scale conversational GPT-based systems exhibits pronounced temporal regularities, with interaction volumes peaking during working hours and on weekdays, and declining during nights and weekends²⁵. Similar seasonality has been documented for data-center workloads more generally, where server utilization follows different daily profiles on weekdays compared to weekends²⁶. These usage patterns imply corresponding periodic variations in computational demand placed on LLM infrastructure. Higher demand typically leads to increased latency and lower throughput, which is undesirable from a user-experience perspective and is therefore actively managed by service providers. To maintain latency within acceptable bounds under high load, providers may employ various load-shedding or efficiency-oriented strategies, such as input compression (e.g., prompt pruning), model compression (e.g., routing requests to quantized models), or inference engine optimization (e.g., sampling from a reduced vocabulary)^{27,28}. While these measures are effective in reducing latency, they can also degrade the quality of generated outputs. Consequently, periodic variations in server load—driven by daily and weekly rhythms of user activity—could translate into systematic, periodic changes in LLM performance.

At the same time, real-world LLM deployments are likely more complex than this simplified picture suggests. Usage patterns vary across countries and time zones, which may smooth or shift aggregate demand peaks. Moreover, providers typically operate multiple geographically distributed data centers rather than a single shared capacity, and requests may be routed dynamically across regions depending on availability, pricing, or failover policies. Additional factors such as autoscaling, heterogeneous hardware, and tiered service levels may further modulate effective capacity. These mechanisms can attenuate or

redistribute temporal effects, but they do not eliminate the possibility that residual periodic structure remains observable at the system level.

In sum, it is theoretically possible that LLM performance may vary systematically over both the day and the week. Crucially, these two rhythms can be expected to be not independent in an additive sense: the daily rhythm is likely to differ between weekdays and weekends, both in amplitude and in shape. This implies that the weekly performance pattern modulates the daily performance pattern rather than simply adding a slowly varying baseline. Hence, we can assume a multiplicative data-generating process—comprising a 24 h daily component and a 7 d weekly modulation, giving rise to an observable performance pattern that should be detectable in an empirical investigation.

1.5 The Present Study

There is theoretical reasoning and growing empirical evidence suggesting that the performance of widely-used LLMs may not be time-invariant, with potentially serious implications for the validity and reproducibility of research on LLM capabilities as well as studies that employ LLMs as research tools. In particular, considerations of how server demand is managed in response to usage patterns suggest that LLM performance may exhibit periodic temporal variability, potentially characterized by a 24-hour rhythm modulated by a 7-day cycle.

Against this background, the present study examines the assumption of time invariance by investigating LLM performance on a fixed task over an extended period of time under fixed conditions. Specifically, we investigate whether model performance shows evidence of the hypothesized periodic temporal patterns.

2 Methods

2.1 Task Selection and Scoring

To measure performance of an LLM over time, we selected a physics task taken from the German Physics Olympiad at an intermediate difficulty level. Pilot tests revealed that this particular task was neither trivial (such that the selected LLM would almost always answer correctly) nor excessively difficult (such that the LLM would almost always answer incorrectly). The task is formulated as a multiple-choice question, meaning that at least one of the listed options is correct. The task—translated from German to English by the authors—reads:

A single battery can power an incandescent bulb for a time t . For simplicity, assume that the bulb shines with constant brightness until the battery is depleted, and that the resistance of the bulb is constant. Which of the following statements are correct if two of these batteries are used to operate two of the bulbs?

- A. If the batteries are connected in series and the bulbs are connected in series, the bulbs can be operated for approximately a time $t/4$.
- B. If the batteries are connected in series and the bulbs are connected in parallel, the bulbs can be operated for approximately a time $t/2$.
- C. If the batteries are connected in parallel and the bulbs are connected in series, the bulbs can be operated for approximately a time $2t$.
- D. If the batteries are connected in parallel and the bulbs are also connected in parallel, the bulbs can be operated for approximately a time t .

Applying basic electrical circuit theory and energy considerations shows that only answer option D is correct.

During pilot tests, we observed that the LLM appeared to evaluate each answer option independently in terms of its plausibility. Accordingly, we adopted an option-wise scoring scheme in which each answer option was evaluated independently. For each option, a score of 0.25 points was awarded for a correct decision—either selecting the option if it is correct or not selecting it if it is incorrect. This procedure yields total scores in the set $\{0, 0.25, 0.5, 0.75, 1\}$. To illustrate, consider the LLM response “B, D”. The response receives 0.25 points for correctly not selecting option A, 0 points for incorrectly selecting option B, 0.25 points for correctly not selecting option C, and 0.25 points for correctly selecting option D, resulting in a total score of 0.5.

2.2 Data Generation Under Fixed Conditions

A specific snapshot of GPT-4o (gpt-4o-2024-08-06) was queried via the OpenAI API (application programming interface) at a fixed temperature setting ($T = 1$) using identical prompting (including system prompt, user prompt, and the introduced multiple-choice physics problem). The API enables programmatic access to OpenAI models from software environments such as Python, allowing recurring queries (e.g., every three hours) to be automated over extended periods of time. This way, ten queries were issued every three hours, beginning on August 5 at 6:00 AM and ending on October 31 at 9:00 PM (in Germany; CEST, UTC+2).

To enable automated scoring of model responses, we enforced a structured output format in which the model returned a JSON object containing (a) the complete solution path and (b) the selected multiple-choice option(s). Automated evaluation was performed solely on the basis of the selected option(s). The multiple-choice task text was provided as the user prompt. The system prompt—translated from German to English by the authors—reads as follows: “You are a physics expert. Solve the problem. Return both the detailed solution path and the final answer in JSON format.” This way, $N = 6,930$ solutions to the problem at hand were generated and automatically scored.

2.3 Data Analysis

All analyses were performed using Python 3.12²⁹.

2.3.1 Analysis of Temporal Drift

To assess whether a systematic performance drift was present in the time-series data, we fitted an ordinary least squares (OLS) regression to the observed values. Statistical inference on the regression coefficients, in particular on the linear drift term, was conducted using Newey–West heteroskedasticity- and autocorrelation-consistent (HAC) standard errors³⁰. This approach provides consistent covariance estimates in the presence of both heteroskedasticity and autocorrelation in the regression residuals, which are common in time-series data. The truncation lag (bandwidth) was selected to cover the longest expected temporal dependence in the data (7 days). Additionally, all measurements were averaged at the daily level and at the weekly level to visually examine potential temporal trends.

2.3.2 Missing Data Handling

Due to unforeseen technical difficulties, data generation was interrupted for a short period. Specifically, no API queries were recorded between October 1, 06:00 and October 2, 06:00 CEST, resulting in nine missing time points, each comprising 10 repeated measurements (which can also be seen by closely looking at Fig. 2a). To handle these missing observations, we applied mean-value imputation using the overall mean of the complete time series, because the missing interval comprises only a small fraction of the total observation window and is therefore unlikely to materially influence estimates of trends, variability, or periodicity, regardless of the specific imputation method used.

2.3.3 Fourier Analysis

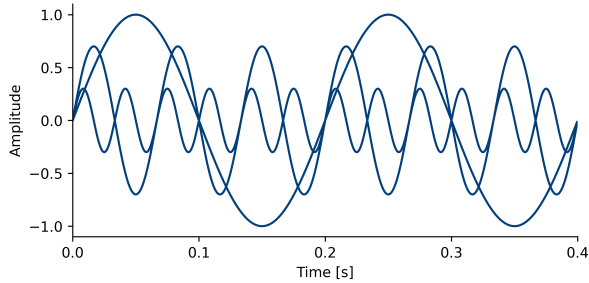
To examine periodic structure in the time series, we performed a Fourier analysis using the fast Fourier transform³¹. The basic principle of Fourier analysis is illustrated in Fig. 1. Consider several periodic components, represented as sinusoidal signals with different frequencies and amplitudes (Fig. 1a). When these components are additively combined, the resulting signal remains periodic but exhibits a more complex waveform, from which the individual constituent frequencies are not readily identifiable by visual inspection alone (Fig. 1b). Fourier analysis addresses this problem by decomposing the observed signal into a weighted sum of sinusoidal basis functions, thereby representing the signal in the frequency domain (Fig. 1c). The Fourier transform thus quantifies the contribution of each frequency component to the overall signal. In practical applications, time series data are typically contaminated by noise, which obscures the underlying periodic structure (Fig. 1d). Nevertheless, Fourier analysis remains capable of identifying dominant periodic components, albeit with reduced precision and increased uncertainty in the presence of noise (Fig. 1e).

In our case, the input data comprised an evenly sampled time series with a fixed temporal resolution of 3 hours, corresponding to a sampling frequency of $f_s = 8$ samples per day. The series spanned an observation period of approximately 87.75 days and, given the fixed sampling interval, consisted of $N = 702$ time points. At each time point, ten individual measurements were available, yielding a total of 7,020 measurement-level data points; missing values at this level were imputed prior to aggregation. The maximum detectable signal frequency (Nyquist frequency) was therefore $f_{\text{Nyq}} = f_s/2 = 4$ cycles per day, corresponding to a minimum resolvable period of 6 hours.

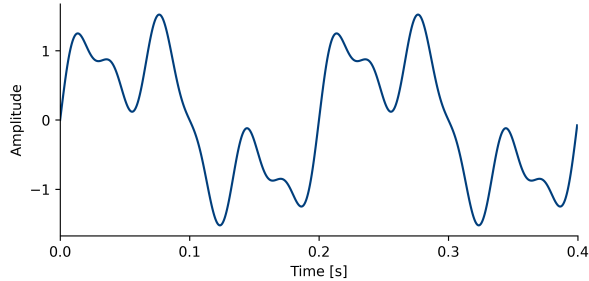
More specifically, power spectra were estimated using Welch’s method³² as implemented in `scipy.signal.welch`³³, because this method provides a robust and low-variance estimate of the power spectrum for finite and potentially noisy time series by averaging spectral estimates across overlapping, windowed segments. This approach reduces sensitivity to random fluctuations and spectral leakage compared to a single discrete Fourier transform.

According to Welch’s method, the time series was segmented into overlapping windows of fixed length ($n_{\text{perseg}} = \lfloor N/4 \rfloor = 175$), with adjacent windows overlapping by 50%. A Hann window was applied to each segment to reduce spectral leakage³⁴, and the resulting segment-wise spectra were averaged to obtain the final spectral estimate. Spectral results are reported in terms of spectral power, corresponding to window-normalized squared Fourier amplitudes. Given a sampling frequency of 8 samples per day and a segment length of 175 samples, the resulting frequency grid had a spacing of approximately 0.05 day^{-1} , which defines the effective frequency resolution of the analysis.

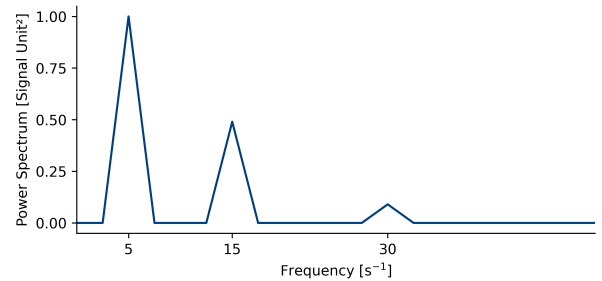
To assess the statistical significance of spectral peaks, we employed a nonparametric permutation procedure^{35,36}. Specifically, the observed time series was randomly permuted $n = 1000$ times to generate surrogate datasets that destroyed temporal



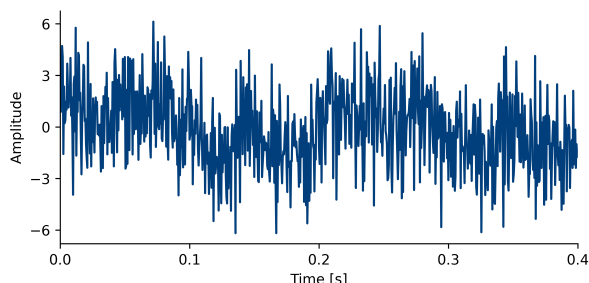
(a) Three sinusoidal signals of the form $x_i(t) = A_i \sin(2\pi f_i t)$ with amplitudes $A_1 = 1.0$, $A_2 = 0.7$, and $A_3 = 0.3$, and frequencies $f_1 = 5 \text{ s}^{-1}$, $f_2 = 15 \text{ s}^{-1}$, and $f_3 = 30 \text{ s}^{-1}$.



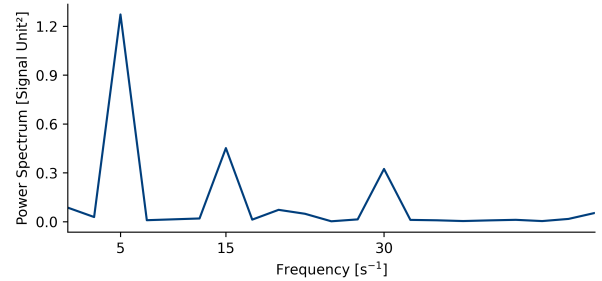
(b) Combined signal $x(t) = x_1(t) + x_2(t) + x_3(t)$ in the time domain.



(c) Power spectrum obtained from the Fourier transform of the combined signal $x(t) = x_1(t) + x_2(t) + x_3(t)$ depicted in Fig. 1b, showing three dominant frequency components at 5 s^{-1} , 15 s^{-1} , and 30 s^{-1} . Peak power equals the squared time-domain amplitude, i.e., $1.0 = 1.0^2$, $0.49 = 0.7^2$, and $0.09 = 0.3^2$.



(d) Noisy combined signal $\tilde{x}(t) = x(t) + \varepsilon(t)$ in the time domain, where $\varepsilon(t) \sim \mathcal{N}(0, \sigma^2)$ with $\sigma = 2$ denotes additive white Gaussian noise.



(e) Power spectrum obtained from the Fourier transform of the noisy combined signal $\tilde{x}(t) = x(t) + \varepsilon(t)$ depicted in Fig. 1d. Compared to Fig. 1c, the noise introduces a broadband background and leads to less sharply defined spectral peaks with time-domain amplitudes that deviate from the actual amplitudes of the underlying sinusoidal components.

Figure 1. Conceptual illustration of how a spectral (Fourier) analysis operates for analyzing time-series data.

dependencies while retaining the distribution of observed values. For each surrogate, the Welch spectrum was recomputed using identical parameters. An empirical significance threshold was then constructed for each frequency bin as the 95th percentile of the bootstrap distribution, corresponding to a one-sided test with $\alpha = 0.05$. Frequencies at which the observed spectrum exceeded this threshold are considered statistically significant.

Following identification of statistically significant spectral peaks, the overall amount of explained variability in performance in the original time series was quantified. Specifically, spectral power is summed over all frequency bins corresponding to statistically significant peak frequencies, and this sum was normalized by the total spectral power. Because the variance of a time series equals the total spectral power³⁷, this procedure yields an estimate of the proportion of variance attributable to periodic components associated with the identified peaks.

In addition to this measure of explained variance, we quantified the time-domain magnitude of variability attributable to the combined periodic components in order to assess how strongly their joint contribution explains fluctuations in the observed performance scores. For this purpose, phase information—unavailable from the Welch power spectrum—was estimated by least-squares fitting of a cosine–sine model to the full time series at each significant frequency. Using these phase estimates together with the corresponding amplitudes, a composite signal was reconstructed by summing all identified periodic components. The reconstructed signal was evaluated over a sufficiently long temporal interval to approximate its asymptotic range.

2.4 Hypothesized Findings

Assuming a multiplicative data-generating process—comprising a 24 h daily periodic pattern and a 7 d weekly modulation—one does not simply expect isolated spectral peaks at 24 h and 7 d in the Fourier spectrum. Because multiplication in the time domain corresponds to convolution in the frequency domain, the resulting Fourier spectrum is obtained by convolving the spectrum of the daily component with that of the weekly component.

Additionally, because the daily performance rhythm is expected to not be sinusoidal, as real-world diurnal processes rarely follow pure sinusoidal dynamics, it will contain harmonics at integer multiples of $f_d = 1 \text{ day}^{-1}$ (e.g., 12 h, 8 h). Likewise, the weekly modulation is expected to be non-sinusoidal due to weekday–weekend asymmetries and will therefore contain a fundamental at $f_w = 1/7 \text{ day}^{-1}$ and its harmonics. Their interaction would therefore produce (more or less observable) spectral components at

$$f = kf_d \pm mf_w,$$

where $f_d = 1 \text{ day}^{-1}$ and $f_w = 1/7 \text{ day}^{-1}$.

In practice, globally deployed LLM services aggregate usage across multiple time zones and regions, each with its own daily and weekly activity profile. This results in a weighted superposition of several phase-shifted and partially heterogeneous periodic signals. While pure phase shifts would not affect the Fourier power spectrum, differences in amplitudes and waveform shapes lead to partial averaging and cancellation. Consequently, spectral peaks are expected to be attenuated or broadened rather than sharply concentrated at the theoretical frequencies. Temporal aggregation may therefore smear the spectrum, but should not eliminate the predicted daily–weekly interaction components.

Thus, if LLM performance is governed by a daily rhythm whose form is modulated across the week, the Fourier spectrum is expected to exhibit not only power near 24 h and 7 d, but also characteristic sidebands at combination frequencies; particularly at $(1/24 \pm 1/168) \text{ h}^{-1}$ for $k = m = 1$, corresponding to periods of approximately 20.6 h and 28.4 h. Importantly, depending on noise, sampling, and the strength of the modulation, these sidebands need not be equally pronounced, and the fundamental 24 h component itself may be weak or even absent. Nevertheless, the presence of one or more such sidebands is the expected spectral consequence of weekly modulation of a daily periodic performance pattern and therefore provides evidence that weekly effects act by reshaping the daily rhythm rather than by introducing an independent weekly fluctuation as in the additive case.

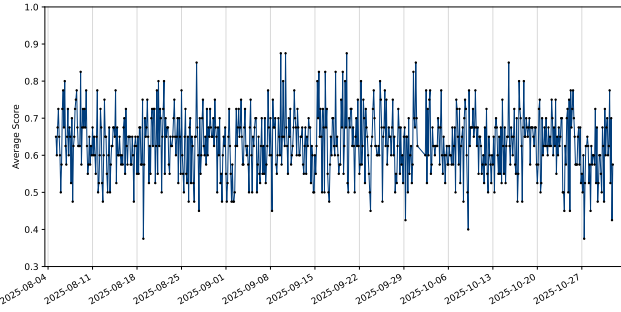
3 Results

3.1 Descriptive Statistics

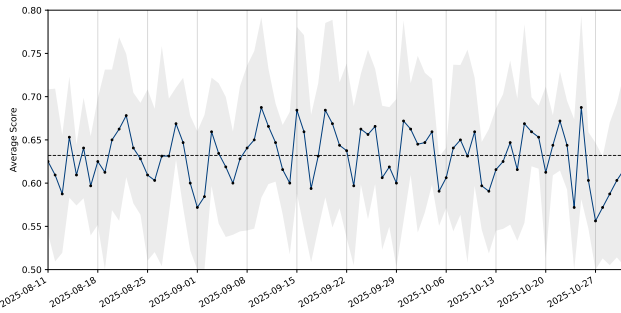
Across all $N = 6,930$ individual measurements, the LLM achieved a mean accuracy of $M = 0.632$ with a standard deviation of $SD = 0.260$. The full range of performance was observed, with both completely correct and completely incorrect responses occurring ($\min = 0$, $\max = 1$). To reduce sampling noise beyond potential systematic periodic variability, the ten observations corresponding to each time point were averaged. This aggregated performance is shown in Fig. 2a. The resulting time series still exhibits substantial variation over the approximately three-month data collection period ($SD_{\text{avg}} = 0.0829$).

3.2 Analysis of Temporal Drift

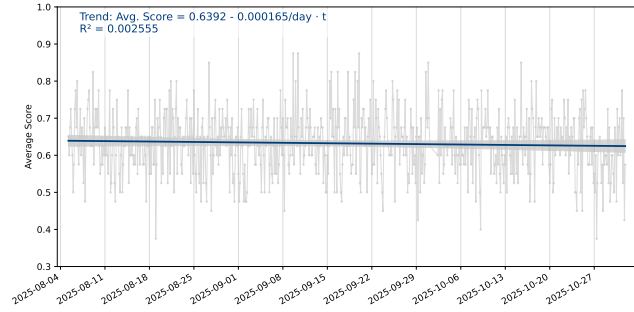
We then fitted an ordinary least squares (OLS) regression with heteroskedasticity- and autocorrelation-consistent (HAC) standard errors to assess whether the time series exhibits a systematic drift (see Fig. 2b). The estimated drift coefficient is



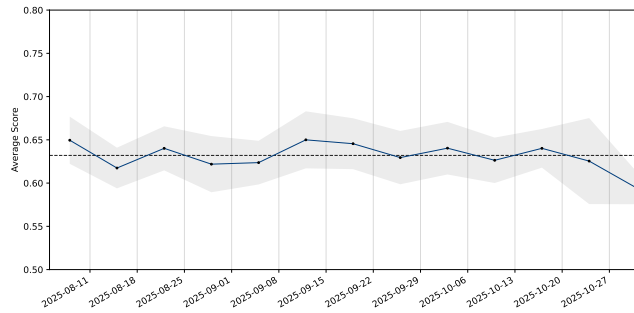
(a) Full time series, with each dot denoting the mean score computed from 10 measurements at the respective time point. All labeled dates on the horizontal axis correspond to Mondays (CEST, UTC+2).



(b) Linear regression line fitted to and overlaid on the full time series shown in Fig. 2a. The shaded band indicates the 95% confidence interval for the estimated mean trend, based on HAC standard errors.



(c) Daily average score over time. Dots represent daily mean scores aggregated from all measurements within each day; the shaded band indicates ± 1 standard deviation. The horizontal dashed line indicates the mean of the time series.



(d) Weekly average score over time. Dots represent weekly mean scores aggregated from all measurements within each week from Monday to Sunday; the shaded band indicates ± 1 standard deviation. The horizontal dashed line indicates the mean of the time series.

Figure 2. Visualization of temporal variability in the score data across different time scales.

1.65×10^{-4} points per day. A t -test based on the HAC standard errors indicates that this estimate does not differ significantly from zero ($t = -1.01$, $p = 0.303$). Accordingly, we find no statistical evidence for a systematic drift across the time from 4 Aug 2025 until 31 Oct 2025 in the data.

We additionally aggregated all measurements at the daily level (see Fig. 2c) and at the weekly level (see Fig. 2d) to visually examine potential temporal trends. The daily average scores shown in Fig. 2c exhibit substantial variability across the week. Although no clear systematic pattern is directly observable, there is a tentative indication that performance tends to be lower around Sunday and Monday, whereas higher scores are observed from Wednesday to Friday. However, fluctuations around this average pattern are considerable, as indicated by the shaded error band. The weekly average scores depicted in Fig. 2d deviate only marginally from the overall mean of the time series, suggesting the absence of periodic patterns beyond the weekly time scale.

To describe weekly and daily variation in performance, and in particular their interaction, we aggregated the data by each combination of weekday and hour of the day. The resulting averages are shown in the heatmap in Fig. 3, together with the corresponding marginal distributions across weekdays and time of day. The heatmap indicates that, over the approximately three-month observation period, the highest average performance is observed on Wednesdays at 09:00 CEST, whereas the lowest average performance is observed on Tuesdays at 03:00 CEST. In addition, the marginal distributions make it possible to revisit the patterns that were only weakly discernible in Fig. 2c and to describe them more clearly. Specifically, average performance is lowest on Mondays, followed by slightly higher but still comparatively low values on Tuesdays. From Wednesday through Saturday, performance remains at a generally higher and relatively stable level, with a small peak on Friday. On Sundays, average performance decreases again to levels comparable to those observed on Mondays. In addition, the marginal distribution across hours of the day provides insight into average daily patterns. However, inspection of the heatmap shows that these daily patterns are not uniform across weekdays. As a consequence, the hourly averages shown in the top marginal plot should be interpreted with caution, as they aggregate over heterogeneous weekday-specific patterns (e.g., weekdays vs. weekend).

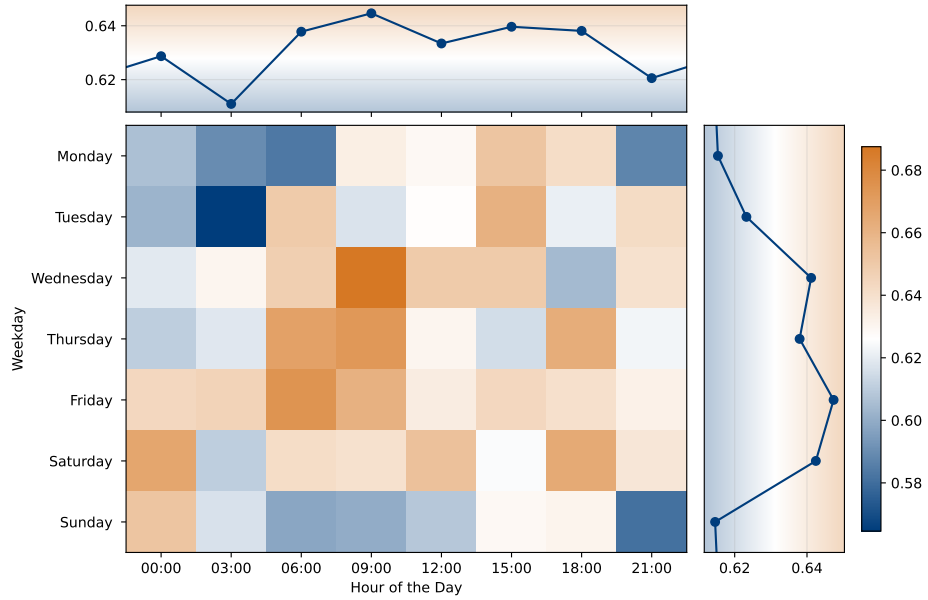


Figure 3. Heatmap of average accuracy as a function of weekday (rows) and time of day (columns), where time of day corresponds to measurement time points taken every three hours. The top panel shows the marginal average accuracy for each time of day, averaged over all weekdays. The right panel shows the marginal average accuracy for each weekday, averaged over all times of day. All times and weekdays are based on Central European Summer Time (CEST, UTC+2).

Notwithstanding this limitation, performance is generally lower during nighttime hours (21:00 to 03:00, CEST) and higher during daytime hours (06:00 to 18:00, CEST).

3.3 Fourier Analysis

To investigate periodic structure in the time series beyond descriptive statistics, we conducted a Fourier analysis using the fast Fourier transform in combination with Welch's method to identify dominant periodic components in the data^{31,32}. Results of the Fourier analysis in the form of a power spectrum are shown in Fig. 4. The spectrum exhibits several distinct peaks that exceed the permutation-based significance threshold, indicating the presence of statistically significant periodic components. Period lengths, frequencies, spectral power, amplitudes, and phase information of all statistically significant peaks are summarized in Table 1.

Two neighboring significant peaks are observed at periods of approximately 5.5 d and 7.3 d, which appear visually as a single broadened peak in the spectrum. This may be attributable to spectral leakage and the limited frequency resolution of the analysis, which prevent a clean separation of closely spaced low-frequency components. Nevertheless, this broadened peak is consistent with the hypothesized periodic weekly component.

Significant peaks are also observed at periods of approximately 30.9 h and 21.0 h. Notably, no dominant peak is detected at exactly 24 h, where a purely daily cycle would be expected. Instead, the observed peaks are located around the 24 h period. This pattern is consistent with sidebands arising from a daily rhythm that is modulated by a weekly cycle, as discussed in section 2.4.

Formally, if a daily component with frequency $f_d = 1 \text{ day}^{-1}$ is multiplicatively modulated by a weekly component with frequency $f_w = 1/7 \text{ day}^{-1} \approx 0.143 \text{ day}^{-1}$, spectral components are expected at frequencies $f = f_d \pm f_w$, corresponding to periods of approximately $(f_d - f_w)^{-1} \approx 28.0 \text{ h}$ and $(f_d + f_w)^{-1} \approx 21.0 \text{ h}$. While the peak at approximately 21.0 h aligns perfectly with the expected upper sideband, the peak at approximately 30.9 h is more offset from the corresponding lower sideband, potentially due to the finite frequency resolution and spectral leakage. Importantly, the absence of a sharp 24 h peak may suggest that the daily effect does not act as an independent, consistently present oscillation. Instead, the strength of the daily pattern seems to vary across the week (as can be seen in Fig. 3). As a consequence, the daily fluctuations may not form a single coherent 24 h pattern across the full observation period, which could substantially reduce the spectral power exactly at 24 h. Nevertheless, because daily variation may still be present in a day-dependent manner (i.e., depending on the day of week), it manifests through the discussed characteristic sidebands around 24 h. Their presence, together with the absence of a sharp 24 h peak, indicates that daily-scale variability is not independent of the weekly cycle but instead varies systematically across the week.

Finally, additional statistically significant peaks are observed at sub-daily periods of approximately 9.6 h and 8.6 h. These

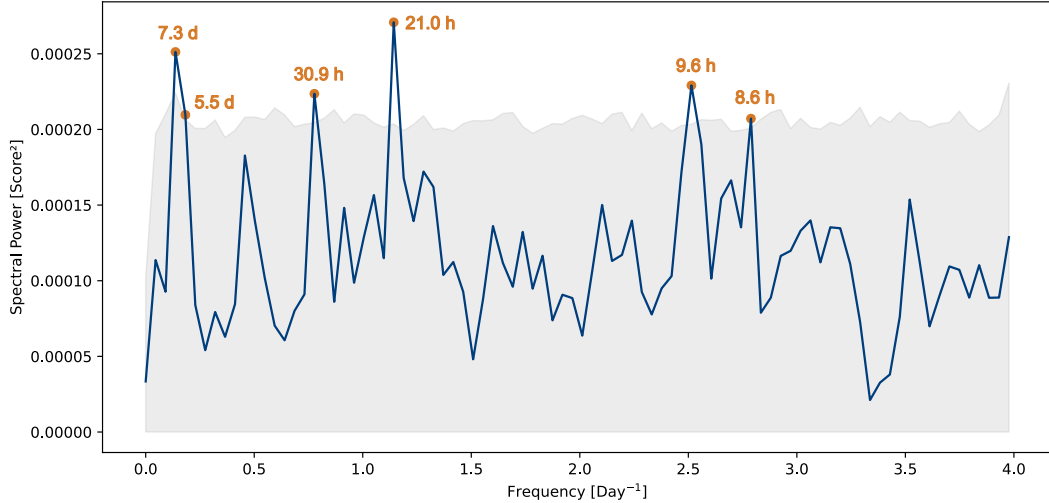


Figure 4. Power spectrum estimated via fast Fourier transformation using Welch's method and Hann-windowing. The grey shaded band indicates the 95% permutation-based significance threshold; labeled spectral peaks exceeding this band are considered statistically significant.

Table 1. Information on the detected significant peaks in the power spectrum shown in Fig. 4. Phase was estimated separately by least-squares sinusoidal fitting at each frequency (cosine reference).

Period Length	Frequency [day ⁻¹]	Spectral Power [score ²]	Amplitude [score]	Phase [degree]
7.3 d	0.137	0.000251	0.0159	35.6
5.5 d	0.183	0.000210	0.0145	-163.6
30.9 h	0.777	0.000224	0.0150	9.8
21.0 h	1.14	0.000271	0.0165	106.7
9.6 h	2.51	0.000229	0.0151	-50.6
8.6 h	2.79	0.000207	0.0144	4.1

faster components may arise because the daily performance rhythm deviates from a purely sinusoidal form (see Fig. 3). In this case, a daily component with frequency $f_d = 1 \text{ day}^{-1}$ generates harmonic contributions at integer multiples $n f_d$. The peak at 9.6 h can arise from modulation sidebands of higher-order harmonics of the daily component. In particular, the second harmonic of the daily rhythm, $2f_d = 2 \text{ day}^{-1}$ (corresponding to a 12 h period), when weakly modulated at the weekly frequency $f_w = 1/7 \text{ day}^{-1}$, produces sidebands at $2f_d \pm f_w = (2 \pm 1/7) \text{ day}^{-1}$, corresponding to periods of approximately 10.6 h and 9.2 h. Given finite frequency resolution and spectral leakage, power associated with these components could plausibly manifest near the observed 9.6 h peak. Similarly, the peak at 8.6 h can be interpreted in terms of the third harmonic $3f_d = 3 \text{ day}^{-1}$ (corresponding to 8 h) of the daily rhythm. If the third harmonic $3f_d = 3 \text{ day}^{-1}$ corresponding to 8 h is weakly modulated by the weekly frequency $f_w = 1/7 \text{ day}^{-1}$, additional sidebands may appear at frequencies $3f_d \pm f_w = (3 \pm 1/7) \text{ day}^{-1}$, corresponding to periods of approximately 7.6 h and 8.4 h, which could plausibly contribute to the observed ≈ 8.6 h peak given finite frequency resolution and spectral leakage. More generally, if the daily rhythm is non-sinusoidal but weak relative to noise, its higher harmonics at $2f_d$ and $3f_d$ may remain below the significance threshold, while modulation by the weekly component shifts part of their spectral power into sidebands at $n f_d \pm f_w$. As a result, a single sideband can become detectable even when the corresponding harmonic peak itself is not, and when the complementary sideband is attenuated or obscured by finite frequency resolution and spectral leakage.

Having identified and interpreted the statistically significant spectral peaks, we next quantify their collective contribution to overall performance variability in the original time series (see Fig. 2a). Specifically, by summing the spectral power $P(f)$ over all frequency bins corresponding to statistically significant peak frequencies f^* , we estimate the proportion of performance variability attributable to periodic components. Because the total variance of a time series equals the integral of its power

spectrum³⁷, this ratio directly reflects the fraction of variance explained by the identified periodic patterns. We compute

$$\text{explained variability} = \frac{\sum_{f^*} P(f)}{SD_{\text{avg}}^2} = \frac{0.001392}{0.0829^2} \approx 20.3\%.$$

These results indicate that approximately 20% of the observed performance variability is associated with the identified periodic components, whereas the remaining variability is not captured by the periodic structure identified here.

In addition to the variance-based analysis, we quantified the aggregate time-domain contribution of the identified periodic components to fluctuations in performance. Using phase estimates obtained via least-squares fitting (see Table 1), we constructed a composite signal by summing all statistically significant periodic components and evaluated it over a sufficiently long temporal interval to approximate its asymptotic range. This procedure yielded a peak-to-peak variation of 0.139 units in the performance score, which is bounded between 0 and 1. Thus, the periodic structure alone accounts for performance swings of approximately 14% of the full scale, indicating that periodic patterns constitute a substantial and practically meaningful source of temporal variability.

4 Discussion

Taken together, our results show that the tested LLM exhibits periodic temporal variability in its performance on the probed physics task, characterized by an interaction between daily- and weekly-scale dynamics. While no dominant 24 h component is observed, the presence of characteristic sidebands around the daily frequency, together with a significant weekly-scale components, is consistent with the hypothesis of a daily performance rhythm whose form varies systematically across the week rather than a mere superposition of independent daily and weekly effects. Additional significant sub-daily peaks can be parsimoniously explained as higher-order consequences of this same interaction in combination with non-sinusoidal daily and weekly rhythms. Quantitatively, the identified periodic components account for approximately 20% of the total observed variability in (average) performance, indicating that a substantial—but not exhaustive—portion of temporal variation follows systematic periodic patterns.

Observed daily fluctuations in performance of LLMs might be interpreted as effects of varying server load; however, such an interpretation requires caution. Our analyses focus on a fixed snapshot of GPT-4o, which is likely deployed on dedicated infrastructure and may not share computational resources with other OpenAI models. Even under the simplifying assumption of a single global server pool serving all GPT-4o users, usage differs across the globe. Usage statistics suggest that ChatGPT usage is dominated by users in North America, particularly the United States and Canada³⁸, where population density is highest along the East and West Coasts. These regions span time zones from UTC-4 (U.S. East Coast) to UTC-7 (U.S. West Coast). If usage follows typical diurnal patterns, global demand would be expected to be lowest during nighttime hours in these regions and generally reduced whenever at least one of the two coasts is at night. Translated to Central European Summer Time (CEST, UTC+2), nighttime on the U.S. East Coast (22:00 to 06:00 local time) corresponds approximately to 04:00 to 12:00 CEST, while nighttime on the U.S. West Coast corresponds to 07:00 to 15:00 CEST. Taking the union of these nighttime intervals—i.e., periods during which at least one major North American population center is asleep—yields a broad window from roughly 04:00 to 15:00 CEST, during which overall North American usage would plausibly be reduced. Consistent with this expectation, our data shows a plateau of increased performance for approximately this window in Germany, as can be seen in the top panel in Fig. 3. Notably, the overlap of nighttime on both coasts—approximately 07:00 to 12:00 CEST—marks a period during which North American usage would be expected to be lowest overall. During this window, European users (particularly in Germany) may therefore experience the highest computational availability per request, which is consistent with the performance maximum observed in our data at 9:00 CEST, as also seen in the upper panel of Fig. 3. Nevertheless, this reasoning remains simplistic and speculative. It does not establish a causal link between server load and observed performance patterns, as such a claim would require more detailed information on global usage distributions, infrastructure-level resource allocation under load, and comparative performance data from additional geographic regions.

Putting aside speculation about the causal mechanisms underlying these effects, our results provide quantitative evidence that periodic temporal variability constitutes a non-negligible source of variability in LLM performance. Specifically, we found that in our context approximately 20% of the total variance in average performance is attributable to periodic components, and that the periodic structure alone induces peak-to-peak performance fluctuations of about 14% of the full performance scale. These magnitudes indicate that temporal effects are not merely statistical artifacts but represent substantively meaningful variation in model behavior over time.

These findings have important implications for the interpretation of performance estimates reported in the existing literature on widely-used LLMs' capabilities. In particular, studies based on data collection restricted to a narrow temporal window may yield biased estimates if that window coincides with periods of systematically elevated or depressed model performance. In such cases, reported performance levels may overstate or understate the true long-run average, respectively. This concern

applies not only to prior empirical studies of LLM capabilities but also to downstream applications that rely on such estimates when deploying LLM-based tools.

When LLMs are used as research tools—for example, in tasks such as deductive qualitative coding or automated annotation—similar considerations apply. In these settings, temporal variability in model performance can introduce systematic biases into research outputs if data collection is confined to limited or unrepresentative time windows. As a result, coding decisions, category assignments, or derived measures may reflect systematic variability in model behavior rather than stable properties of the underlying data or coding scheme. This risk is particularly salient when LLM outputs are treated as fixed or objective inputs to subsequent analyses, as the temporal variability may propagate downstream and affect substantive research conclusions.

Importantly, our results do not imply that conclusions drawn in earlier studies on or using LLMs are invalid. Rather, they highlight an additional and previously underappreciated source of uncertainty: sampling decisions in time. Temporal sampling choices can meaningfully affect final performance estimates, yet this source of variability has rarely been explicitly considered or quantified in prior work. As a consequence, existing estimates of LLM performance should be interpreted with greater uncertainty than is typically acknowledged.

To increase the validity and reproducibility of research on or using LLMs, greater attention to data collection procedures is necessary. In particular, with respect to the overall duration of data collection, measurements should span at least one full week, corresponding to the longest periodicity identified in our data. Covering this seven-day interval is necessary to obtain an unbiased estimate of mean performance across the periodic components of the signal. Within this window, measurements should also be taken at a sufficiently fine temporal resolution to capture higher-frequency periodicities in addition to the weekly cycle. To be conservative, we therefore recommend an hourly measurement schedule. When measurements are evenly spaced across a full week, this design enables reliable estimation of average performance while accounting for periodic temporal structure. In addition to adequate temporal coverage, multiple measurements per time point are required to address sampling noise arising from the stochastic nature of LLM outputs. Even after accounting for periodic effects, a substantial proportion of the observed variability in our study—approximately 80%—could not be attributed to temporal periodicity. To reduce this remaining variability, as many repetitions per time point as feasible should be collected, subject to practical constraints such as computational cost and evaluation effort. Notably, even with 10 measurements per time point, approximately 80% of the variability in our data remained attributable to sampling noise, suggesting that, in general, more than 10 measurements per time point may be warranted. We acknowledge that these recommendations imply a large number of LLM outputs for a single task (e.g., 7 days \times 24 measurements per day \times 10 repetitions = 1680 measurements). However, when outputs are evaluated automatically—as is standard practice in most benchmark studies—this does not pose substantial feasibility concerns. Beyond reporting means or modal assignments derived from the full measurement period, we further recommend reporting measures of variability (e.g., standard deviations) or visualizing full output distribution. When such statistics are used in downstream analyses, explicitly incorporating and propagating this uncertainty is likely to be beneficial.

The present study has some limitations that also point to clear avenues for future research. First, the temporal sampling procedure was limited in resolution. Measurements were taken only every three hours, which constrains the ability to resolve higher-frequency components of the daily rhythm and increases the risk of aliasing in the spectral analysis. In addition, at each time point the LLM was only queried ten times to solve the specific task at hand, which does introduce sampling variability into the estimated performance signal. Future studies should therefore sample more frequently (e.g., hourly or sub-hourly) and increase the number of repeated measurements per time point in order to obtain a more accurate and finely resolved estimate of the underlying performance pattern. Second, our analysis was restricted to a single class of tasks—solving a multiple-choice physics problem. To assess the generality of the observed periodicities, the same methodology should be applied to a broader range of tasks and contexts, including other scientific domains, creative tasks, and instruction-following scenarios. Third, while we interpret the observed daily and weekly patterns in terms of infrastructure-level load management and efficiency-oriented inference strategies, this does not account for a causal explanation of the observed temporal variability in performance. A crucial next step is therefore to compare externally hosted LLMs from different providers, which may implement different load-balancing and optimization schemes, as well as to contrast them with locally hosted models that run without shared server-side load. If the periodic structure is driven primarily by server load and load-shedding mechanisms, it should be attenuated or absent in locally deployed models and should differ systematically across external services. More broadly, respective findings may motivate a shift toward offline, locally hosted models where feasible, as such deployments offer greater control over execution conditions and can help ensure the reproducibility and temporal stability of LLM-based analyses.

We close the discussion by noting that periodic temporal variability in performance is not unique to LLMs but is also well documented in human cognition and judgment. In this sense, a human researcher conducting qualitative analyses may likewise perform differently across time, following temporal patterns that may not be fundamentally different from those observed in this study for LLM performance. Empirical research has shown that human cognitive performance varies both within a day and across a week as a function of circadian rhythms, time awake, and cumulative fatigue, affecting attention, executive control,

and judgment consistency even in expert populations^{39,40}. Accordingly, human judgments often exhibit periodic temporal variability driven by biological and contextual factors. For example, judicial decision-making has been shown to depend on time since the last break, with favorable rulings occurring more frequently immediately after breaks than just before them⁴¹. Similarly, qualitative research has highlighted persistent challenges in reproducing coding decisions across studies, even when formalized rubrics are employed, illustrating that human evaluative outputs can remain temporally and contextually variable despite attempts at strict standardization⁴². A key distinction between human and machine decision-making, however, lies in metacognitive monitoring: humans can, at least in principle, reflect on and regulate their own cognitive states, even though such monitoring is imperfect and itself state dependent. LLMs, by contrast, lack any capacity for self-monitoring or awareness of fluctuations in their own performance, implying that temporally variability—once present—cannot be internally detected or compensated for by the system itself. In this fundamental respect, humans retain a decisive advantage.

Acknowledgements

The authors are grateful to their colleagues for valuable discussions regarding reproducibility standards in AI-based research. They particularly thank Dietmar Block for insightful and constructive discussions on spectral analysis.

Author contributions statement

PT: study conception and design, data collection, analysis, interpretation, and manuscript preparation. PW: study conception and design, data collection, and manuscript preparation.

Additional information

Competing interests: The authors declare no competing interests.

Data Availability

The data along with the analysis code are available in an OSF repository: <https://doi.org/10.17605/OSF.IO/PFYQ4>

References

1. Brown, T. B. *et al.* Language models are few-shot learners. *arXiv* DOI: [10.48550/ARXIV.2005.14165](https://doi.org/10.48550/ARXIV.2005.14165) (2020).
2. Naveed, H. *et al.* A comprehensive overview of large language models. *ACM Transactions on Intell. Syst. Technol.* **16**, 1–72, DOI: [10.1145/3744746](https://doi.org/10.1145/3744746) (2025).
3. Kortemeyer, G. Could an artificial-intelligence agent pass an introductory physics course? *Phys. Rev. Phys. Educ. Res.* **19**, 010132, DOI: [10.1103/PhysRevPhysEducRes.19.010132](https://doi.org/10.1103/PhysRevPhysEducRes.19.010132) (2023).
4. Yeadon, W. & Hardy, T. The impact of AI in physics education: A comprehensive review from GCSE to university levels. *Phys. Educ.* **59**, 025010, DOI: [10.1088/1361-6552/ad1fa2](https://doi.org/10.1088/1361-6552/ad1fa2) (2024).
5. Aldazharova, S., Issayeva, G., Maxutov, S. & Balta, N. Assessing AI’s problem solving in physics: Analyzing reasoning, false positives and negatives through the force concept inventory. *Contemp. Educ. Technol.* **16**, ep538, DOI: [10.30935/cedtech/15592](https://doi.org/10.30935/cedtech/15592) (2024).
6. Kortemeyer, G., Babayeva, M., Polverini, G., Widenhorn, R. & Gregorcic, B. Multilingual performance of a multimodal artificial intelligence system on multisubject physics concept inventories. *Phys. Rev. Phys. Educ. Res.* **21**, DOI: [10.1103/98hg-rkrf](https://doi.org/10.1103/98hg-rkrf) (2025).
7. Wang, X. *et al.* SciBench: Evaluating college-level scientific problem-solving abilities of large language models, DOI: [10.48550/arXiv.2307.10635](https://doi.org/10.48550/arXiv.2307.10635) (2024). [2307.10635](https://doi.org/10.48550/arXiv.2307.10635).
8. Feng, K. *et al.* PHYSICS: Benchmarking foundation models on university-level physics problem solving, DOI: [10.48550/ARXIV.2503.21821](https://doi.org/10.48550/ARXIV.2503.21821) (2025).
9. Phan, L. *et al.* Humanity’s last exam, DOI: [10.48550/ARXIV.2501.14249](https://doi.org/10.48550/ARXIV.2501.14249) (2025).
10. Than, N., Fan, L., Law, T., Nelson, L. K. & McCall, L. Updating “The future of coding”: Qualitative coding with generative large language models. *Sociol. Methods & Res.* **54**, 849–888, DOI: [10.1177/00491241251339188](https://doi.org/10.1177/00491241251339188) (2025).
11. Xiao, Z., Yuan, X., Liao, Q. V., Abdelghani, R. & Oudeyer, P.-Y. Supporting qualitative analysis with large language models: Combining codebook with GPT-3 for deductive coding. In *28th International Conference on Intelligent User Interfaces*, 75–78, DOI: [10.1145/3581754.3584136](https://doi.org/10.1145/3581754.3584136) (ACM, Sydney NSW Australia, 2023).

12. VERBI Software. Maxqda – the art of data analysis. <https://www.maxqda.com> (2025).
13. Jansen, T. *et al.* Data extraction by generative artificial intelligence: Assessing determinants of accuracy using human-extracted data from systematic review databases. *Psychol. Bull.* **151**, 1280–1306, DOI: [10.1037/bul0000501](https://doi.org/10.1037/bul0000501) (2025).
14. OpenAI. GPT-5 System Card. Tech. Rep. (2025).
15. Zhang, Y. *et al.* Exploring the role of large language models in the scientific method: From hypothesis to discovery. *npj Artif. Intell.* **1**, 14, DOI: [10.1038/s44387-025-00019-5](https://doi.org/10.1038/s44387-025-00019-5) (2025).
16. Wulff, P., Kubsch, M. & Krist, C. Natural language processing and large language models. In Wulff, P., Kubsch, M. & Krist, C. (eds.) *Applying Machine Learning in Science Education Research: When, How, and Why?*, 117–142 (Springer Nature Switzerland, Cham, 2025).
17. Chang, T. A. & Bergen, B. K. Language model behavior: A comprehensive survey. *Comput. Linguist.* **50**, 293–350, DOI: [10.1162/coli_a_00492](https://doi.org/10.1162/coli_a_00492) (2024).
18. Tu, S. *et al.* Chatlog: Carefully evaluating the evolution of chatgpt across time. *arXiv* (2024).
19. Ignjatović, A. *et al.* Chatgpt’s progress over time: A longitudinal enhancing biostatistical problem-solving in medical education. *Heal. informatics journal* **31**, 14604582251381260, DOI: [10.1177/14604582251381260](https://doi.org/10.1177/14604582251381260) (2025).
20. Dai, H., Teehan, R. & Ren, M. Are llms prescient? a continuous evaluation using daily news as the oracle. *arXiv* (2025).
21. Chen, L., Zaharia, M. & Zou, J. How is chatgpt’s behavior changing over time? *Harv. Data Sci. Rev.* **6**, DOI: [10.1162/99608f92.5317da47](https://doi.org/10.1162/99608f92.5317da47) (2024).
22. Does chatgpt get better /worse at different times of the day? (when under load.). Reddit, r/ChatGPTPro (2026). Accessed 2026-01-16.
23. Gupta, M., Virostko, J. & Kaufmann, C. Large language models in radiology: Fluctuating performance and decreasing discordance over time. *Eur. J. Radiol.* **182**, 111842, DOI: [10.1016/j.ejrad.2024.111842](https://doi.org/10.1016/j.ejrad.2024.111842) (2025).
24. Tschigale, P. *et al.* Evaluating gpt- and reasoning-based large language models on physics olympiad problems: Surpassing human performance and implications for educational assessment. *arXiv* **abs/2505.09438**, DOI: [10.48550/ARXIV.2505.09438](https://doi.org/10.48550/ARXIV.2505.09438) (2025).
25. Wang, Y. *et al.* BurstGPT: A real-world workload dataset to optimize LLM serving systems. In *Proceedings of the 31st ACM SIGKDD Conference on Knowledge Discovery and Data Mining* V.2, 5831–5841, DOI: [10.1145/3711896.3737413](https://doi.org/10.1145/3711896.3737413) (ACM, Toronto ON Canada, 2025).
26. Landré, D., Philippe, L. & Pierson, J.-M. Seasonal study of user demand and IT system usage in datacenters. In *2024 IEEE 30th International Conference on Parallel and Distributed Systems (ICPADS)*, 693–702, DOI: [10.1109/ICPADS63350.2024.00095](https://doi.org/10.1109/ICPADS63350.2024.00095) (IEEE, Belgrade, Serbia, 2024).
27. Miao, X. *et al.* Towards efficient generative large language model serving: A survey from algorithms to systems. *ACM Comput. Surv.* **58**, 1–37, DOI: [10.1145/3754448](https://doi.org/10.1145/3754448) (2025).
28. Zhou, Z. *et al.* A Survey on efficient inference for large language models, DOI: [10.48550/arXiv.2404.14294](https://doi.org/10.48550/arXiv.2404.14294) (2024). [2404.14294](https://doi.org/10.48550/arXiv.2404.14294).
29. Python Software Foundation. *Python 3.12 Reference Manual*. Python Software Foundation, 3.12 edn. (2023). Accessed: 2026-01-21.
30. Newey, W. K. & West, K. D. A simple, positive semi-definite, heteroskedasticity and autocorrelation consistent covariance matrix. *Econometrica* **55**, 703, DOI: [10.2307/1913610](https://doi.org/10.2307/1913610) (1987). [1913610](https://doi.org/10.2307/1913610).
31. Cochran, W. *et al.* What is the fast Fourier transform? *Proc. IEEE* **55**, 1664–1674, DOI: [10.1109/PROC.1967.5957](https://doi.org/10.1109/PROC.1967.5957) (1967).
32. Welch, P. The use of fast Fourier transform for the estimation of power spectra: A method based on time averaging over short, modified periodograms. *IEEE Transactions on Audio Electroacoustics* **15**, 70–73, DOI: [10.1109/TAU.1967.1161901](https://doi.org/10.1109/TAU.1967.1161901) (1967).
33. Virtanen, P. *et al.* SciPy 1.0: Fundamental algorithms for scientific computing in python. *Nat. Methods* **17**, 261–272, DOI: [10.1038/s41592-019-0686-2](https://doi.org/10.1038/s41592-019-0686-2) (2020).
34. Prabhu, K. M. M. *Window Functions and Their Applications in Signal Processing* (CRC Press, Boca Raton, 2018), 1 edn.
35. Odell, R. H., Smith, S. W. & Eugene Yates, F. A permutation test for periodicities in short, noisy time series. *Annals Biomed. Eng.* **3**, 160–180, DOI: [10.1007/BF02363068](https://doi.org/10.1007/BF02363068) (1975).

36. Ptitsyn, A. A., Zvonic, S. & Gimble, J. M. Permutation test for periodicity in short time series data. *BMC Bioinforma.* **7**, S10, DOI: [10.1186/1471-2105-7-S2-S10](https://doi.org/10.1186/1471-2105-7-S2-S10) (2006).
37. Oppenheim, A. V. & Schafer, R. W. *Discrete-Time Signal Processing*. Prentice Hall Signal Processing Series (Prentice Hall, Upper Saddle River, New Jersey, 1999), 2 edn.
38. Bailyn, E. ChatGPT usage statistics: January 2026 (2026).
39. Hannon, B. & Dunlop, D. The influences of day of the week on cognitive performance. *Br. J. Educ. Soc. & Behav. Sci.* **16**, 1–11, DOI: [10.9734/BJESBS/2016/26784](https://doi.org/10.9734/BJESBS/2016/26784) (2016).
40. Schmidt, C., Collette, F., Cajochen, C. & Peigneux, P. A time to think: Circadian rhythms in human cognition. *Cogn. Neuropsychol.* **24**, 755–789, DOI: [10.1080/02643290701754158](https://doi.org/10.1080/02643290701754158) (2007).
41. Danziger, S., Levav, J. & Avnaim-Pesso, L. Extraneous factors in judicial decisions. *Proc. Natl. Acad. Sci. United States Am.* **108**, 6889–6892, DOI: [10.1073/pnas.1018033108](https://doi.org/10.1073/pnas.1018033108) (2011).
42. O'Connor, C. & Joffe, H. Intercoder reliability in qualitative research: Debates and practical guidelines. *Int. J. Qual. Methods* **19**, DOI: [10.1177/1609406919899220](https://doi.org/10.1177/1609406919899220) (2020).